

# Solution measurement of DNA curvature in papillomavirus E2 binding sites

Jeff M. Zimmerman and L. James Maher III\*

Department of Biochemistry and Molecular Biology, Mayo Clinic-Rochester, 200 First Street SW, Rochester, MN 55905, USA

Received April 18, 2003; Revised and Accepted July 3, 2002

## ABSTRACT

**'Indirect readout' refers to the proposal that proteins can recognize the intrinsic three-dimensional shape or flexibility of a DNA binding sequence apart from direct protein contact with DNA base pairs. The differing affinities of human papillomavirus (HPV) E2 proteins for different E2 binding sites have been proposed to reflect indirect readout. DNA bending has been observed in X-ray structures of E2 protein–DNA complexes. X-ray structures of three different E2 DNA binding sites revealed differences in intrinsic curvature. DNA sites with intrinsic curvature in the direction of protein-induced bending were bound more tightly by E2 proteins, supporting the indirect readout model. We now report solution measurements of intrinsic DNA curvature for three E2 binding sites using a sensitive electrophoretic phasing assay. Measured E2 site curvature agrees well the predictions of a dinucleotide model and supports an indirect readout hypothesis for DNA recognition by HPV E2.**

## INTRODUCTION

Sequence-specific DNA recognition by proteins is a fundamental feature of DNA packaging, recombination and gene expression. DNA site discrimination by proteins reflects free energy release due to the combination of: (i) enthalpically favorable protein–DNA contacts; (ii) entropically favorable release of bound water and cations; and (iii) favorable or unfavorable energetics of conformational changes in the two partners. Direct recognition of base-specific hydrogen bond donor and acceptor arrays is often fundamental to site discrimination. Hydrogen bonding at specific sites minimizes energy penalties associated with hydrogen bond donor–donor and acceptor–acceptor clashes. Because of the frequent requirement for conformational changes upon binding, there is evidence that the local shape or flexibility of the DNA sugar–phosphate backbone contributes to the energetics of binding site selection. Such sequence-dependent DNA recognition without base contacts has been termed 'indirect readout'.

Indirect readout was initially proposed to explain DNA site discrimination by the bacterial *trp* repressor where base-specific contacts within the cognate binding site are conspicuously absent (1). An analysis of thermodynamic and structural correlations relevant to indirect readout has been presented for a set of protein–DNA complexes (2). The human papillomavirus (HPV) E2 proteins have recently been proposed to exemplify indirect readout in their discrimination among E2 binding sites in the viral genome (3). Papillomaviruses are DNA tumor viruses, many of which infect humans and other mammals. While HPV strains 6 and 11 are associated with common warts, other strains including HPV-16 and HPV-18 appear to be causative factors in cervical carcinoma (3). Among viral gene products, the regulatory E2 proteins are important dimeric DNA binding proteins involved in the regulation of viral gene transcription and genome replication (3). HPV E2 proteins recognize DNA via a unique dimeric  $\beta$ -barrel motif within the DNA binding domain, linked to activation domains by poorly conserved linker domains of 40–200 amino acids.

E2 binding sites occur as variations of the sequence 5'-ACCGNNNCGGT in duplex DNA. Multiple E2 binding sites exist in all papillomavirus genomes. These sequences conserve the  $N_4$  spacing in the recognition sequence, but the  $N_4$  sequence itself is variable. In a detailed initial study, it was shown that (i) the nature of the  $N_4$  sequence determines HPV-16 E2 protein binding affinity and (ii) protein binding is accompanied by DNA bending (4). In particular, HPV-16 E2 binding affinity is relatively low for the  $N_4$  spacer 5'-ACGT, is 8-fold higher for the  $N_4$  spacer 5'-TTAA and is 33-fold higher for the  $N_4$  spacer 5'-AATT (5).

Because the  $N_4$  spacer sequence influences HPV E2 binding affinity, it was logical to presume that critical protein–DNA contacts involve these bases. It was therefore puzzling when X-ray structures of E2 protein–DNA complexes (6) revealed that no base-specific contacts are made with the central  $N_4$  sequence (Fig. 1A) (reviewed in 3). E2 binding site DNA is bent by 40–50° in the various co-crystals and the general features of the complexes do not depend on the particular  $N_4$  sequence present. Base-specific recognition occurs in two consecutive major grooves, with bending into the intervening minor groove (Fig. 1A). It has, therefore, been proposed that the intrinsic shape or flexibility of the  $N_4$  non-contacted spacer within the E2 binding site plays an indirect role in determining

\*To whom correspondence should be addressed. Tel: +1 507 284 9041; Fax: +1 507 284 2053; Email: maher@mayo.edu

Respectfully dedicated to the memory of Claude Hélène



the average mobility of each group of five ligation products sharing the same duplex insert, but containing the five different right arms, according to:

$$\mu_{\text{rel}} = \mu / \mu_{\text{avg}} \quad 1$$

where  $\mu_{\text{rel}}$  is the relative mobility,  $\mu$  is the mobility of each ligation product (in mm) and  $\mu_{\text{avg}}$  is the average mobility of a group of probes sharing the same duplex insert.

The value of  $\mu_{\text{rel}}$  was plotted against the spacing (in bp) between the center of the E2 site (inserts **1–3**) or proximal  $A_5$  tract (inserts **c0–c3**) and the center of the 5'  $A_5$  tract in R-A to R-E. Data were then fit using KaleidaGraph™ software to the phasing function (12):

$$\mu_{\text{rel}} = (A_{\text{PH}} / 2) \{ \cos[2\pi(S - S_{\text{T}}) / P_{\text{PH}}] \} + 1 \quad 2$$

where  $A_{\text{PH}}$  is the amplitude of the phasing function,  $S$  is the normalized spacer length,  $S_{\text{T}}$  is the *trans* spacer length and  $P_{\text{PH}}$  is the phasing period (set at 10.5 bp/turn). The value of  $A_{\text{PH}}$  estimated from curve fitting is related to the magnitude of curvature in the synthetic insert. The value of  $S_{\text{T}}$  estimated from curve fitting allows evaluation of the direction of insert duplex curvature relative to the phased  $A_5$  tract array intrinsic to the right arm.

### DNA curvature estimates

The empirical relationship between DNA curvature and phasing amplitude is established using duplex insert standards containing zero to three phased  $A_5$  tracts. This relationship is linear, providing a standard curve for extracting DNA curvature estimates (in degrees of helix axis deflection). This standard curve is based on an assumption of 18° of static helix axis deflection per  $A_5$  tract, with curvature toward the minor groove viewed in a reference frame set one half of a base pair 3' from the center of the  $A_5$  tract.

## RESULTS AND DISCUSSION

### Experimental design

The structural details of an HPV E2 protein–DNA complex are shown in Figure 1A. Key recognition base pairs (gold) flank the central non-contacted  $N_4$  sequence (yellow). Our approach to measuring the intrinsic shape of various E2 binding sites involves calibration of an electrophoretic phasing assay with standard DNAs whose curvature is due to zero to three phased  $A_5$  tracts (Fig. 1B, duplexes **c0**, **c1**, **c2**, **c3**). These duplexes are individually tested by ligation between ~100 bp DNA arms 'L' and 'R-A' through 'R-E' (Fig. 1C) in an *in vitro* trimolecular ligation facilitated by appropriate unique DNA cohesive termini (9). The resulting DNA probes systematically alter the spacing between an array of three phased  $A_5$  tracts in the right arms 'R-A' through 'R-E' and elements of curvature in the inserted synthetic duplex, I (Fig. 1C). To assess E2 binding site shape, DNA duplexes **1–4** were synthesized (Fig. 1B). Duplex **1** contains a high-affinity E2 binding site whose minor groove at the center of the  $N_4$  spacer is in phase with two adjacent  $A_5$  tracts. Duplexes **2** and **3** (Fig. 1B) contain similar arrangements including a medium-affinity (duplex **2**) or

low-affinity (duplex **3**) E2 binding site. Control duplex **4** (Fig. 1B) contains two phased  $A_5$  tracts and no E2 binding site.

Electrophoretic phasing assays exploit the observation that intrinsic DNA curvature (or anisotropic flexibility) reduces gel mobility. Systematic alteration of helical phasing between two elements of curvature in DNA will alter the global DNA shape from a fast-migrating 'S-shaped' conformation to a slow-migrating 'C-shaped' conformation. Analysis of gel mobility as a function of helical phasing for standards of known intrinsic curvature (typically provided by  $A_{5-6}$  tracts) provides an empirical relationship between phasing amplitude and DNA curvature. This relationship can be used to assign curvature estimates to new DNA sequences (9).

### Prediction of E2 site intrinsic shape

Prior X-ray crystallography studies have suggested intrinsic curvature for certain E2 binding sites (7,8). Before analysis in solution, we implemented the optimized dinucleotide bending model of Liu and Beveridge (10) to visualize calculated trajectories of the three 12 bp E2 sequences in duplexes **1–4** (Fig. 1B), flanked by intrinsically straight DNA sequences (tandem direct repeats of arbitrary 5 bp segments). For each input sequence, a single DNA structural representation is produced by this algorithm. It is important to note that this 'structure' is a representation of both DNA curvature and flexibility.

This dinucleotide model algorithm predicts significant differences in the shapes of the various E2 binding sites. The results are shown in Figure 2. The high-affinity E2 binding site in duplex **1** is predicted to be curved by ~17° toward the minor groove at the center of the  $N_4$  sequence (Fig. 2). In the medium-affinity sequence in duplex **2**, the curvature angle is predicted to be 8° in the same direction. The low-affinity E2 binding site in duplex **3** is predicted to be curved by only 3° toward the minor groove, and the corresponding 12 bp non-E2 sequence in duplex **4** is predicted to be straight (Fig. 2). It is striking that these curvature predictions correspond well to expectations for affinity rankings based on the extent to which pre-existing DNA curvature simulates the bent DNA conformation in the E2–protein complex.

### Solution detection of DNA curvature

Trimolecular ligations and phasing assays were performed using native polyacrylamide gels to monitor DNA shape by mobility changes. The results of an initial calibration experiment are shown in Figure 3A. Each group of five lanes shows ligation products derived from the indicated duplex insert (see Fig. 1B) and different right arms. Inspection of the data reveals that increasing the number of phased  $A_5$  tracts increases the amplitude of the electrophoretic migration anomaly. Relative mobility was plotted as a function of phasing distance and fit to a conventional phasing function as described in Materials and Methods. The result is shown in Figure 4A. When the phasing amplitudes derived from these data fits were plotted against the total expected DNA curvature for these standards (assuming the conventional value of 18° of curvature per  $A_5$  tract), a linear relationship was obtained (Fig. 4B). Similar results have been obtained previously (9). This simple function allows the sensitive estimation of DNA curvature

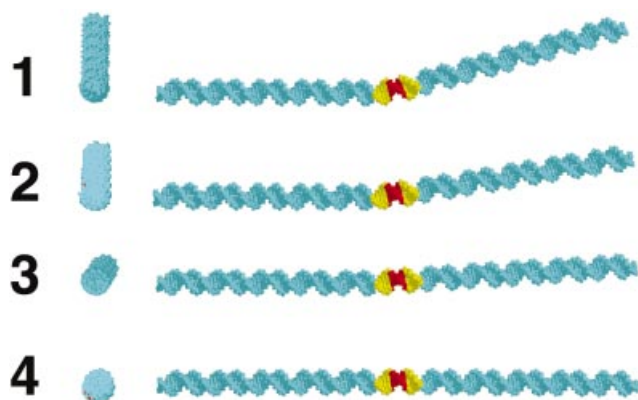


**Figure 2.** Predicted DNA curvature. Molecular models depict end views (left) and side views (right) of the 12 bp E2 recognition sites of inserts 1–4, positioned between 56 bp segments of intrinsically straight DNA. Structures were predicted by the Liu–Beveridge model (10) (see Materials and Methods). Atoms corresponding to the E2 recognition sites and  $N_4$  spacers sequence are shown in gold and red, respectively.

for an unknown sequence when it is substituted in the position of the proximal  $A_5$  tract of the test array.

Electrophoretic experiments were repeated for duplexes 1–4 (Fig. 1B) and the raw data are shown in Figure 3B. Fitting of the data to the phasing function is shown in Figure 4C, and the resulting DNA shape estimates are shown in Table 1. Duplex 4 contains two phased  $A_5$  tracts and no E2 binding site. Its estimated absolute curvature was  $28^\circ$  (reflecting the presence of two phased  $A_5$  tracts), so this value was subtracted in all cases to produce net curvature estimates. As shown in Table 1, the estimated E2 site curvatures are significantly different for the three E2 sites with different  $N_4$  spacers. The most curved is the E2 site containing the 5′-AATT spacer (duplex 1). The curvature estimate for this duplex is  $17.8^\circ$ , which compares favorably with the curvature of  $17^\circ$  predicted by the Liu–Beveridge dinucleotide model (Fig. 2). Table 1 shows that duplex 2 has a lower curvature,  $11.2^\circ$ , similar to the  $8^\circ$  prediction (Fig. 2). Neither duplex 3 (E2 site with 5′-ACGT spacer) nor 4 (no E2 site) displayed significant curvature (Table 1). These results again are similar to predictions of the Liu–Beveridge model.

Table 1 also lists the curvature direction, a fitting parameter that reflects the horizontal position of the minima and maxima of the cosine function in phasing graphs such as Figure 4C. The curvature direction is similar in all cases ( $\sim 22$  bp) and is within 1 bp of the standard construct in which two arrays of three  $A_5$  tracts are maximally aligned. This confirms that the measured curvature is in the expected direction, i.e. toward the minor groove at the center of the E2 sequence.

Because the 5′-AATT and 5′-ACGT sequences have previously been examined by X-ray crystallography both alone (7,8) and in complex with E2 proteins (reviewed in 3), it is possible to directly compare our ‘low-resolution’ solution measurements of DNA shape with these prior reports. Both studies agree that the low-affinity site containing the 5′-ACGT sequence is minimally curved. For the high-affinity E2 site containing the 5′-AATT sequence, X-ray crystallography showed three duplex forms with an average curvature of  $\sim 10^\circ$ . Our solution curvature estimate for this sequence is  $\sim 18^\circ$ .

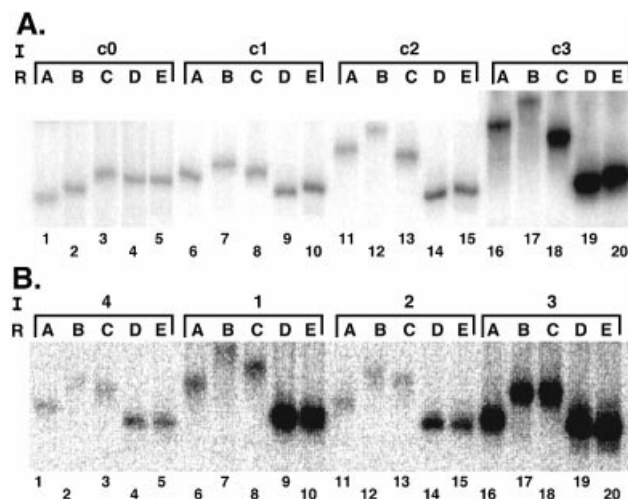


**Figure 3.** Semi-synthetic phasing analysis of intrinsic DNA curvature. (A) DNA curvature analysis with the indicated standard inserts (I) containing zero to three phased  $A_5$  tracts ligated to the left DNA arm and the indicated right arm (R). (B) Phasing analysis for inserts 1–4 (see Fig. 1) containing E2 binding sites with different spacer sequences.

Possible explanations for the difference include the different experimental conditions and the absence of a crystal environment. Both methods concur that the intrinsic curvature direction for the high-affinity site is as expected, i.e. toward the minor groove at the center of the E2 binding site. Our work goes beyond prior high resolution studies by also providing a shape estimate for the intermediate-affinity E2 binding site with 5′-TTAA spacer. In accord with its intermediate affinity, the site has an apparent intermediate curvature of  $\sim 11^\circ$ .

It is important to note that we have, by convention, interpreted electrophoretic retardation by both our  $A_5$  tract standards and E2 test sequences in terms of static curvature. This is supported by the X-ray structure of an E2 site containing 5′-AATT spacer (8) where static curvature is observed. Nonetheless, electrophoretic measurements cannot distinguish between static curvature and anisotropic flexibility. Thus, it cannot formally be excluded that the E2 sites containing 5′-AATT and 5′-TTAA sequences are not intrinsically curved, but display variable propensities to deformation toward the minor groove at the center of the non-contacted central spacer. Whether static curvature or anisotropic flexibility, the case remains that an intrinsic physical property of DNA in the non-contacted region of E2 sites correlates with observed binding affinity.

Recently, detailed all-atom molecular dynamics simulations have been undertaken by Byun and Beveridge to examine a series of DNA constructs comparable with those studied here (13). The concordance between these simulations and the results of crystallography and the solutions measurements reported here is compelling.

As both DNA curvature estimates and equilibrium E2 protein binding affinities become available, it may be possible to predict (or rationalize) the E2 protein binding affinity for each variant E2 site by estimating the free energy cost of DNA deformation from its intrinsic (free) state to the bent conformation in the protein complex. This cost would appear as a penalty in estimating equilibrium dissociation constants for the corresponding protein–DNA complexes. It would be



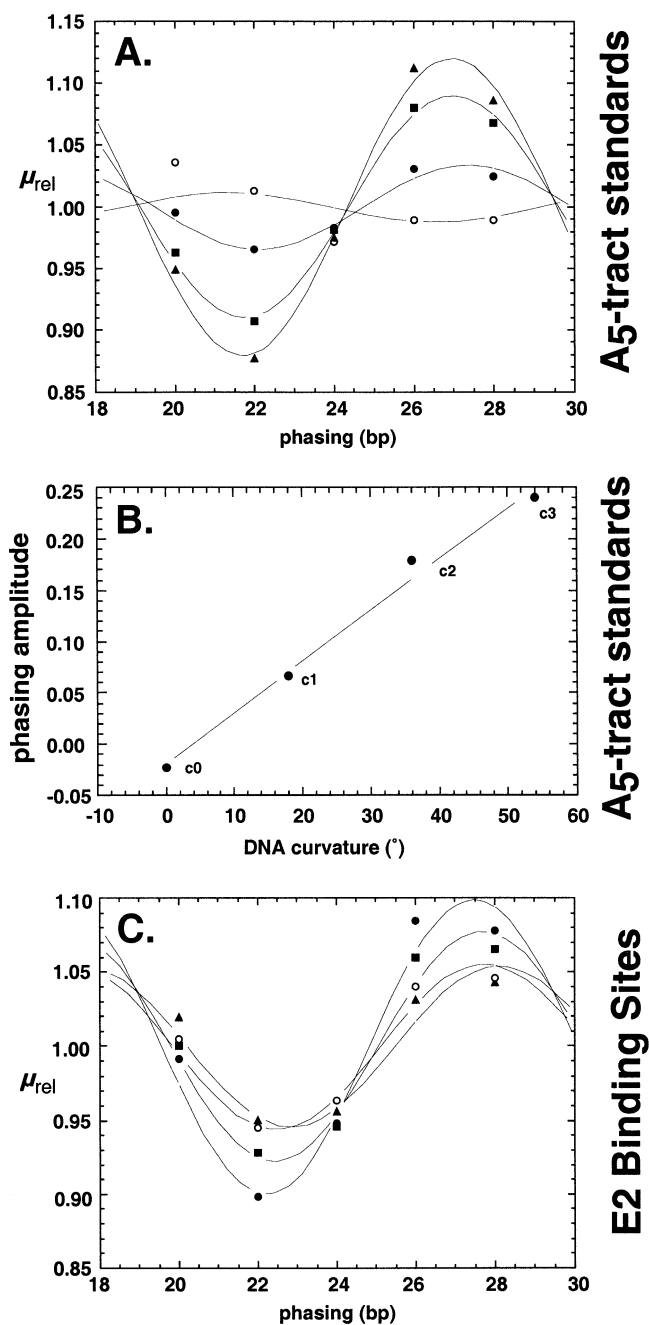


**Figure 4.** Quantitative analysis of phasing data. (A) Plot of  $\mu_{rel}$  (defined in Materials and Methods) as a function of phasing between zero (c0; open circles), one (c1; closed circles), two (c2; closed squares) or three (c3; closed triangles) phased  $A_5$  tracts in the insert and the array of three phased  $A_5$  tracts in the right arm. Fitting to equation 2 is as described in Materials and Methods. (B) Calibration of the linear relationship between intrinsic DNA curvature and phasing amplitude for inserts c1–c3. (C) Phasing data for analysis of E2 binding site inserts 1 (closed circles), 2 (closed squares), 3 (closed triangles) and 4 (open circles).

predicted that the lowest-affinity spacers would be intrinsically curved toward the major groove at the center of the binding site (i.e. the ‘wrong’ direction with respect to the protein complex), while the highest affinity sites will be, as shown here, most intrinsically curved toward the central minor groove.

**Table 1.** E2 site DNA curvature in solution

Insert ( $N_4$ )	E2 site net curvature <sup>a</sup> (°)	Curvature direction <sup>b</sup> (bp)
1 (AATT)	$17.8 \pm 1.2$	$22.26 \pm 0.10$
2 (TTAA)	$11.2 \pm 2.5$	$22.42 \pm 0.01$
3 (ACGT)	$1.2 \pm 3.0$	$22.88 \pm 0.06$
4	0	$22.45 \pm 0.03$

<sup>a</sup>DNA curvature relative to insert 4. Curvature estimates were obtained as described in Materials and Methods. Curve fitting of phasing data to equation 2 allowed extraction of a phasing amplitude for each construct. Using phasing amplitudes for phased  $A_5$  tract reference standards and an assumption of  $18^\circ$  curvature per  $A_5$  tract, amplitudes were converted to degrees of DNA curvature. The reported E2 site curvature was obtained by subtracting the absolute curvature of insert 4 ( $\sim 28^\circ$ ) from curvature estimates for inserts 1–4. Data are averages  $\pm$  standard deviations based on two experiments.

<sup>b</sup>The curvature direction is defined as the base pair spacing (arbitrary reference frame) separating the E2 test sequence in the insert duplex from the phased  $A_5$  tract array in the right phasing arms, that gives rise to the minimum mobility (maximum curvature, hence maximal alignment of loci of curvature). For  $A_5$  tract standards, this parameter has a value of 21.85 bp. The observation that this reference frame remains within  $\sim 1$  bp from the center of the E2 site indicates curvature in the expected direction. Deviation from the value of 21.85 bp observed for  $A_5$  tracts can also reflect a subtle difference in the helical repeat parameter for the E2 binding sequence relative to the corresponding sequence in insert 4.

Interestingly, bovine papillomavirus (BPV) E2 proteins are similar to HPV E2 proteins and bind the same E2 sites; BPV E2 proteins reportedly show little discrimination between sites on the basis of  $N_4$  sequences (5). This observation shows that subtle features of a DNA–protein complex may influence the importance of indirect readout in binding energetics.

## CONCLUSIONS

Our data support a model in which the binding affinity of HPV-16 E2 proteins for variant E2 binding sites reflects an energy balance between the favorable free energy release associated with the protein–DNA interaction and the unfavorable free energy cost of altering the conformation of the E2 binding site DNA to allow protein interaction. In this simple model, E2 binding sites whose intrinsic shapes better approximate the DNA conformation in the E2 protein–DNA complex suffer smaller energy penalties for DNA deformation and enjoy larger residual binding energies. Such sites are therefore observed to be bound with higher affinities by E2 proteins. The electrophoretic measurements reported here tend to corroborate the results of X-ray crystallography (7,8) and support the predictive dinucleotide model of Liu and Beveridge (10,14).

## ACKNOWLEDGEMENTS

The authors acknowledge the staff of the Mayo Molecular Biology Core Facility for technical assistance, R. Hegde and P. Hardwidge for discussion and encouragement, and N. Becker for comments on the manuscript. We thank K. Byun and D. Beveridge for discussion and for sharing their unpublished results. This work was supported by the Mayo Foundation and NIH grant GM54411 to L.J.M.

## REFERENCES

1. Otwinowski,Z., Schevitz,R.W., Zhang,R.G., Lawson,C.L., Joachimiak,A., Marmorstein,R.Q., Luisi,B.F. and Sigler,P.B. (1988) Crystal structure of *trp* repressor/operator complex at atomic resolution. *Nature*, **335**, 321–329.
2. Jen-Jacobson,L., Engler,L.E. and Jacobson,L.A. (2000) Structural and thermodynamic strategies for site-specific DNA binding proteins. *Struct. Fold Des.*, **8**, 1015–1023.
3. Hegde,R.S. (2002) The papillomavirus E2 proteins: structure, function and biology. *Annu. Rev. Biophys Biomol. Struct.*, **31**, 343–360.
4. Bedrosian,C.L. and Bastia,D. (1990) The DNA-binding domain of HPV-16 E2 protein interaction with the viral enhancer: protein-induced DNA bending and role of the nonconserved core sequence in binding site affinity. *Virology*, **174**, 557–575.
5. Hines,C.S., Meghoo,C., Shetty,S., Biburger,M., Brenowitz,M. and Hegde,R.S. (1998) DNA structure and flexibility in the sequence-specific binding of papillomavirus E2 proteins. *J. Mol. Biol.*, **276**, 809–818.
6. Kim,S.S., Tam,J.K., Wang,A.F. and Hegde,R.S. (2000) The structural basis of DNA target discrimination by papillomavirus E2 proteins. *J. Biol. Chem.*, **275**, 31245–31254.
7. Rozenberg,H., Rabinovich,D., Frolow,F., Hegde,R.S. and Shakked,Z. (1998) Structural code for DNA recognition revealed in crystal structures of papillomavirus E2-DNA targets. *Proc. Natl Acad. Sci. USA*, **95**, 15194–15199.
8. Hizver,J., Rozenberg,H., Frolow,F., Rabinovich,D. and Shakked,Z. (2001) DNA bending by an adenine–thymine tract and its role in gene regulation. *Proc. Natl Acad. Sci. USA*, **98**, 8490–8495.
9. Hardwidge,P.R., Zimmerman,J.M. and Maher,L.J.,III (2000) Design and calibration of a semi-synthetic DNA phasing assay. *Nucleic Acids Res.*, **28**, E102.
10. Liu,Y. and Beveridge,D.L. (2001) A refined prediction method for gel retardation of DNA oligonucleotides from dinucleotide step parameters: reconciliation of DNA bending models with crystal structure data. *J. Biomol. Struct. Dyn.*, **18**, 505–526.
11. Sayle,R.A. and Milner-White,E.J. (1995) RASMOL: biomolecular graphics for all. *Trends Biochem. Sci.*, **20**, 374.
12. Kerppola,T.K. and Curran,T. (1991) DNA bending by Fos and Jun: the flexible hinge model. *Science*, **254**, 1210–1214.
13. Byun,K.S. and Beveridge,D.L. (2003) Molecular dynamics simulations of papillomavirus E2 DNA sequences: dynamical models of oligonucleotide structures in solution. *Biopolymers*, in press.
14. Hardwidge,P.R. and Maher,L.J. (2001) Experimental evaluation of the Liu-Beveridge dinucleotide step model of DNA structure. *Nucleic Acids Res.*, **29**, 2619–2625.